THE JOURNAL OF BIOLOGICAL CHEMISTRY
Vol. 276, No. 3, Issue of January 19, pp. 1742–1749, 2001

Printed in U.S.A.

Sites of Phosphorylation by Protein Kinase A in CDC25Mm/GRF1, a Guanine Nucleotide Exchange Factor for Ras*

Received for publication, June 30, 2000, and in revised form, September 15, 2000
Published, JBC Papers in Press, October 3, 2000, DOI 10.1074/jbc.M005770200

Soria Baouz‡§¶, Eric Jacquet‡¶‖, Katia Accorsi‡, Codjo Hountondji‡‡, Monica Balestrini§§, Renata Zippel§§, Emmapaola Sturani§§, and Andrea Parmeggiani‡ ¶¶**

From the ‡Groupe de Biophysique-Equipe 2, Ecole Polytechnique, 91128 Palaiseau Cedex, France, ‡‡Laboratoire de Biochimie, UMR 7654 du CNRS, Ecole Polytechnique, 91128 Palaiseau Cedex, France, and §§Dipartimento di Fisiologia e Biochimica Generali, Università degli Studi di Milano, Via Celoria 26, 20133 Milano, Italy

Activation of the neuronal Ras GDP/GTP exchange factor (GEF) CDC25Mm/GRF1 is known to be associated with phosphorylation of serine/threonine. To increase our knowledge of the mechanism involved, we have analyzed the ability of several serine/threonine kinases to phosphorylate CDC25Mm *in vivo* and *in vitro*. We could demonstrate the involvement of cAMP-dependent protein kinase (PKA) in the phosphorylation of CDC25Mm in fibroblasts overexpressing this RasGEF as well as in mouse brain synaptosomal membranes. *In vitro*, PKA was found to phosphorylate multiple sites on purified CDC25Mm, in contrast to protein kinase C, calmodulin kinase II, and casein kinase II, which were virtually inactive. Eight phosphorylated serines and one threonine were identified by mass spectrometry and Edman degradation. Most of them were clustered around the Ras exchanger motif/PEST motifs situated in the C-terminal moiety (residues 631–978) preceding the catalytic domain. Ser^{745} and Ser^{822} were the most heavily phosphorylated residues and the only ones coinciding with PKA consensus sequences. Substitutions S745D and S822D showed that the latter mutation strongly inhibited the exchange activity of CDC25Mm on Ha-Ras. The multiple PKA-dependent phosphorylation sites on CDC25Mm suggest a complex regulatory picture of this RasGEF. The results are discussed in the light of structural and/or functional similarities with other members of this RasGEF family.

Ras proteins are molecular switches cycling between the active GTP-bound and the inactive GDP-bound forms (1). They control a series of physiological and pathological events associated with growth and differentiation of the cell. Their activity is regulated by GTPase-activating proteins (GAPs)[1] that enhance the intrinsic GTPase activity and by guanine nucleotide exchange factors (GEFs) that accelerate the very slow intrinsic GDP/GTP exchange, favoring thus the regeneration of the active form of Ras. The nucleotide exchange mechanism catalyzed by GEFs has been intensively studied and characterized at a three-dimensional structural level (for review, see Ref. 2). Diverse RasGEFs have been identified: SOS1 and SOS2, RasGRP, CDC25Mm/GRF1, and GRF2. SOS1 and SOS2 are ubiquitary GEFs and their activation depends on signals from tyrosine kinase receptors (for review, see Ref. 3). RasGRP is a neuronal RasGEF involved in diacylglycerol and calcium regulation of Ras (4, 5). CDC25Mm/GRF1 has been shown to be activated by heterotrimeric G protein coupled receptors, such as muscarinic receptors (6, 7); it is predominantly expressed in the neuronal cell and is involved in calcium-associated signals (8, 9). The highly homologous GRF2 is present in cells from different organs (10) and shows *in vivo* functional differences from GRF1 (11). In brain extracts, the GRF1/GRF2 heterooligomer formation was observed (12). These GEFs are modular proteins containing specific domains. CDC25Mm, a protein of 1262 amino acid residues, shows the following sequence of domains/motifs: pleckstrin homology 1 (PH1), coiled-coil (CC), ilimaquinone (IQ), Dbl homology (DH), pleckstrin homology 2 (PH2), Ras exchanger motif (REM), and PEST. The RasGEF domain, represented by the conserved catalytic CDC25 domain, is situated in the C-terminal region.

Results *in vitro* with CDC25Mm (13) and *in vivo* with SOS (14) indicated that the N-terminal portion of GEF down-regulates the activity of the catalytic domain. Several reports have shown that activation of CDC25Mm is coupled with Ca^{2+} influx, as well as with formation of a complex with calmodulin and phosphorylation (8, 15). The latter modification was found to concern serine/threonine (6, 16) and very recently also tyrosine residues (17). The nonreceptor tyrosine kinase Src can induce on CDC25Mm a Rac1-GEF activity (18), showing that this protein is an important element for cross-regulation of Ras and Rac-dependent pathways (19), as has been reported for SOS (20) and GRF2 (21). Taken together, these results illus-

* This work was supported by Contracts BIO4-CT98-0297 and BIO4-CT96-1110 from the European Community, by the Ligue Nationale Française Contre le Cancer, by the Association pour la Recherche sur le Cancer, and by the Italian Consiglio Nazionale delle Ricerche, Projetto Finalizzato Biotecnologie. The costs of publication of this article were defrayed in part by the payment of page charges. This article must therefore be hereby marked "*advertisement*" in accordance with 18 U.S.C. Section 1734 solely to indicate this fact.

§ Present address: IRSC-CNRS, Laboratoire d'oncologie virale, UPR 9045, 94801 Villejuif Cedex, France.

¶ These two authors contributed equally to this work.

‖ Present address: Laboratoire de Synthèse Organique, UMR 7652 du CNRS, Département de Chimie, Ecole Polytechnique, 91128 Palaiseau Cedex, France.

** Present address: Dipartimento di Biotecnologie e Bioscienze, Università degli Studi di Milano-Bicocca, 20126 Milano, Italy.

¶¶ To whom correspondence should be addressed. Tel.: 33-169333298, Fax: 33-169333004; E-mail: andrea@pmc.polytechnique.fr.

[1] The abbreviations used are: GAP, GTPase-activating protein; GEF, GDP/GTP exchange factors; ME, 2-mercaptoethanol; PKA, protein kinase A; PKC, protein kinase C; CaMKII, calmodulin kinase II; CKII, casein kinase II; MBP, maltose-binding protein; 8-Br-cAMP, 8-bromoadenosine-3′,5′-cyclic monophosphate; PDBu, phorbol dibutyrate; PAGE, polyacrylamide gel electrophoresis; RIPA, radioimmune precipitation assay; PCR, polymerase chain reaction; MALDI, matrix-assisted laser desorption-ionization; GRF, guanine nucleotide releasing factor; REM, Ras exchanger motif; IQ, ilimaquinone; DH, Dbl homology; PH, pleckstrin homology; CC, coiled-coil; HPLC, high performance liquid chromatography.

trate the complexity of the upstream activation of CDC25Mm, as well as the many aspects that remain to be clarified.

In order to deepen our information on the specific action(s) of kinases on CDC25Mm, in this work we have carried out a series of experiments analyzing the phosphorylation of this GEF by several serine/threonine kinases. PKA was found to be a very efficient phosphotransfer enzyme for CDC25Mm *in vivo* and *in vitro*, leading to the phosphorylation of multiple residues that were identified by matrix-assisted laser desorption-ionization (MALDI) mass spectrometry and Edman degradation. Functional modifications induced by phosphorylation of full-length CDC25Mm and by substitutions of single serine residues are also reported.

EXPERIMENTAL PROCEDURES

Materials—[γ-^{32}P]ATP (111 Tbq/mmol) was from PerkinElmer Life Sciences; the PKA catalytic subunit, PKC, and casein kinase II were from Roche Molecular Biochemicals; and calmodulin kinase II was from Calbiochem.

CDC25Mm Mutagenesis—Mutants CDC25Mm(S745A) and (S745D) were constructed using a megaprimer PCR method, *Pwo* polymerase (Roche Molecular Biochemicals) and the gene fragment encoding the C-terminal CDC25Mm half-molecule (pGEX-CDC25Mm-(631–1262)), as template. The first step used oligonucleotide CCGTCGGAAGCTG-**G**CCCTCAACATCCCC (S745A) or CCGTCGGAAGCTG**GA**CCTCAA-CATCCCC (S745D) as a mutagenic primer and CCTGGAGCCT-GAGAGCTCCCCAGG as a second primer hybridizing 200 bases downstream on the CDC25Mm open reading frame. The resulting products together with ^{719}GTTGTATGACGCTCTTGATGTTG^{741}, as a second primer hybridized to pGEX, was used for the next PCR step. The obtained fragment carrying the substitution was *Bam*HI-*Sac*I-digested and introduced in pGEX-CDC25Mm-(631–1262), of which the *Eco*RI-*Eco*RI fragment was cloned into pGEX-CDC25Mm. Its *Bam*HI-*Sal*I fragment was cloned in pMal-c2, yielding the gene for the mutated MBP-fused CDC25Mm. CDC25Mm(S822A) and CDC25Mm(S822D) were also obtained by PCR using pGEX-CDC25Mm-(631–1262) as template. CCTGGGGAGCTCTCAGCCTCCAGGAAGCAT**GCA**TCTGAT-GTC (S822A) or CCTGGGGAGCTCTCAGCCTCCAGGAAGCAT**GA**CT-CTGATGTC (S822D) containing a *Sac*I site were the mutagenic primers, while ^{1261}GGGGTTCCGCGCACATTTCCCC^{1249} hybridizing to pGEX was the second primer. The PCR products digested with *Nde*I-*Sac*I were inserted in pGEX-CDC25Mm. The *Bam*HI-*Sal*I fragment from these vectors was subcloned in pMal-c2, leading to the genes encoding MBP-CDC25Mm(S822A) and MBP-CDC25Mm(S822D). In order to exclude secondary mutations, the sequence of the mutants was carried out with an ABI-Prism Sequencer (model 377) over all the mutagenized or inserted fragments.

The CDC25Mm fragments isolated, *i.e.* CDC25Mm-(1–239) (PH1-CC-IQ), CDC25Mm-(239–480) (DH), CDC25Mm-(239–591) (DH-PH2), CDC25Mm-(1–630) (N-terminal half-molecule), CDC25Mm-(631–1262) (C-terminal half-molecule), and CDC25Mm-(978–1262) (RasGEF catalytic domain), were constructed by PCR methods to be described in detail elsewhere. For CDC25Mm-(1–239), CDC25Mm-(239–480), and CDC25Mm-(239–591), pMal vectors were used; for the remaining constructs, pGEX vectors were used.

Expression and Purification of Recombinant CDC25Mm Proteins and of Isolated Domains Thereof—The full-length CDC25Mm proteins and fragments were produced in *Escherichia coli* SCS-1 strain. The bacteria were grown at 30 °C in 1.5 liters of LB medium containing 50 μg/ml ampicillin. Expression of the glutathione *S*-transferase- and MBP-fused proteins were induced at 24 °C at a cell density of 0.2 A_{600} units by adding isoprpyl-1-thio-β-D-galactopyranoside (0.1 mM), and the incubation was continued to 1.5–2.0 A_{600} units. The cell culture, chilled to 4 °C, was centrifugated at 5,000 $\times$ *g* for 10 min and the pellet resuspended in 10 ml of 25 mM Tris-HCl, pH 7.5, 50 mM NaCl, 10% glycerol, 7 mM ME, and 0.5 mM Pefabloc-SC. After sonication (five times for 15 s each), the suspension was centrifuged at 25,000 $\times$ *g* for 20 min at 4 °C and the supernatant was mixed batchwise with 5 ml of glutathione-Sepharose 4B (Amersham Pharmacia Biotech) or 5 ml of amylose resin (New England Biolabs), and gently shaken for 30 min at 4 °C, as reported previously (13, 22). The resin was washed four times with 25 mM Tris-HCl, pH 7.5, 50 mM NaCl, 7 mM ME and the protein eluted with glutathione (3 mg/ml) or maltose (10 mM) solutions in the same buffer. Concerning the MBP fusions with full-length CDC25Mm and CDC25Mm-(631–1262), a second purification step on HiTrap heparin column was carried out. The purification pattern was the same for both wild-type and mutant proteins. Purified proteins were concentrated with Aquacide II (Calbiochem), except for full-length CDC25Mm to avoid aggregation phenomena, and dialyzed against 50 mM Tris-HCl, pH 7.5, 50 mM NaCl, 50% glycerol, and 7 mM ME. When stored at −20 °C in this buffer, the recombinant proteins were stable for at least several months. The CDC25Mm-(1–1262) protein preparation contained approximately 50% full-length product, the remaining proteins consisting of N-terminal shorter fragments of CDC25Mm (13). The various isolated N-terminal CDC25Mm fragments were more than 90% pure. The catalytic domain CDC25Mm-(978–1262) was isolated and purified to homogeneity as described (22).

Cell Culture and CDC25Mm Immunoblotting—The clone NIHRG7 overexpressing CDC25Mm was described in Ref. 7. Subconfluent monolayers of clone NIHRG7 were serum-starved for 24 h and stimulated with forskolin as indicated. Cells were then washed with ice-cold phosphate-buffered saline, extracted in SDS-sample buffer, electrophoresed on SDS-PAGE, and blotted with Ras-GRF antibodies from Santa Cruz. Immunostaining was visualized with ECL (Amersham Pharmacia Biotech).

Phosphorylation of CDC25Mm from Fibroblasts and Synaptosomal Membranes from Mouse Brain—NIHRG7 fibroblasts stimulated with forskolin were washed with phosphate-buffered saline and scraped in 1 ml of ice-cold RIPA buffer (20 mM Tris-HCl, pH 7.4, 150 mM NaCl, 1% Triton X-100, 1% sodium deoxycholate, 0.1% SDS, 10 mM NaF, 0.1 mM Na_3VO_4, 1 mM phenylmethylsulfonyl fluoride, 10 μg/ml leupeptin, 10 μg/ml aprotinin). The lysate was centrifuged for 10 min at 14,000 $\times$ *g* and precleared by incubation with protein A-Sepharose coated with preimmune antiserum. Supernatants were incubated (2 h at 4 °C) with 30 μl of protein A-Sepharose previously coupled with 20 μl of Ras-GRF-specific antiserum (αCF2, Ref. 23). Sepharose beads were washed twice with kinase buffer and incubated in phosphorylation mixture containing 30 mM Tris-HCl (pH 7.4), 10 mM $MgCl_2$, 1 mM dithiothreitol, 2 μM ATP, 370 KBq of [γ-^{32}P]ATP, and 25 units of the catalytic subunit of beef heart PKA (a kind gift of Paolo Tortora, University of Milano-Bicocca, Milan, Italy) for 20 min at 30 °C. The samples, washed three times in RIPA buffer, were analyzed by SDS-PAGE and quantified for autoradiography by densitometric scanning.

The synaptosomal membranes were prepared from mouse brain according to Ref. 24 as reported previously (Ref. 25 (see in particular Fig. 2, fraction LP1)). The washed synaptosomal fraction was hypotonically lysed by resuspension in lysis buffer (10 mM HEPES, pH 7.4, 1 mM EDTA, 1 mM dithiothreitol) containing protease inhibitors. After 30 min in ice, the suspension was centrifuged for 20 min at 40,000 rpm in a Beckman 50 Ti rotor and the supernatant discarded. The pellet was resuspended in lysis buffer and centrifuged. The final synaptosomal membrane fraction was resuspended in phosphorylation buffer (25 mM HEPES, pH 7.4, 1 mM EDTA, 1 mM EGTA) to a final protein concentration of 2 mg/ml. Aliquots (200 μg) were incubated for 5 min at 30 °C (final volume, 200 μl) in phosphorylation buffer in the presence of 10 mM $MgCl_2$ and 10 μM ATP, 370 KBq of [γ-^{32}P]ATP plus 10 mM 8-bromo-cAMP, 1.5 mM $CaCl_2$, or 1.5 mM $CaCl_2$ with 200 nM PDBu. The incubation mixture was then suspended in RIPA buffer and CDC25Mm was immunoprecipitated with Ras-GRF antibodies (Santa Cruz) and subjected to SDS-PAGE and autoradiography.

Phosphorylation of Purified CDC25Mm—Labeling of CDC25Mm with kinases were performed by incubating reaction mixtures of recombinant CDC25Mm with PKA, PKC, CaMKII, or casein kinase II and [γ-^{32}P]ATP (33 Bq/pmol), at 30 °C, in the appropriate buffer, as recommended by the manufacturers. The quantification of ^{32}P incorporation was carried out in two ways. Aliquots (15 μl) of the phosphorylation mixture were heated to 100 °C for 5 min in SDS-sample loading buffer and resolved on SDS-PAGE (8–10%). The labeled proteins were visualized by autoradiography, and ^{32}P was quantified by excising the corresponding bands from dried gels and counting their radioactivity in a liquid scintillation counter (Amersham Pharmacia Biotech, model Wallac 1410). A fragment of similar size was excised from a ^{32}P-free portion of the gel and its radioactivity subtracted. As an alternative method, an aliquot (15 μl) of the phosphorylation reaction was transferred to glass fiber filters (Whatman GFA), which were incubated in cold 10% trichloroacetic acid, 200 mM phosphoric acid. The filters were first washed in the same solution at room temperature, then twice in a mixture ethanol/ether (1/1 v/v), and finally in ether. They were dried and transferred to scintillation vials, and the radioactivity was counted.

Purification of Phosphopeptides—The phosphorylation mixture (500 μl) containing 250 milliunits of PKA, 1000 pmol of CDC25Mm-(631–1262), 50 mM Tris-HCl, pH 7.5, 5 mM $MgCl_2$, 1 mM dithiothreitol, and 100 μM [γ-^{32}P]ATP (33 Bq/pmol) was incubated at 30 °C for 1 h and dialyzed against 50 mM ammonium acetate (pH 8.0). The ^{32}P-labeled

CDC25Mm-(631–1262) was digested overnight at 37 °C with $TosPheCH_2Cl$-treated trypsin (Sigma) at a 1/20 protease to substrate ratio (w/w). The tryptic digest was vacuum-dried, resuspended in 10 μl of electrophoresis buffer, pH 4.4, containing pyridine/acetic acid/H_2O (1/10/189 v/v/v), and spotted onto a TLC plate (Polygram Cell 300 UV254, 20 × 20 cm, 0.1 mm; Macherey-Nagel). Peptides were separated in the first dimension by electrophoresis at 500 V, 120 mA in the buffer mentioned above and in the second dimension by chromatography in buffer pH 3.4 containing pyridine/1-butanol/acetic acid/H_2O (50/75/15/60, v/v/v/v). Peptides were visualized with fluorescamine spray (10 mg/100 ml of acetone), and the position of the radiolabeled phosphopeptides was determined by autoradiography. The labeled peptides were recovered from cellulose with 30% acetic acid and lyophilized. Lyophilizates were dissolved in 0.1% (v/v) trifluoroacetic acid and injected onto a RPLC C18 column (Vydac 150 × 2.1 mm, particles of 5 μm) equilibrated with 0.1% trifluoroacetic acid in water (v/v). Peptides were eluted with linear gradients of acetonitrile in 0.1% (v/v) trifluoroacetic acid at a flow rate of 1 ml/min. Peaks were detected by recording absorbance at 215 nm as well as by radioactivity measurements in a liquid scintillation counter.

Mass Spectrometry Analysis of Phosphopeptides—Mass spectra of phosphopeptides were recorded on a matrix-assisted laser desorption-ionization time-of-flight mass spectrometer. Samples analyzed by MALDI mass spectrometry were prepared by mixing 1.5 μl of matrix (saturated solution of α-cyano-4-hydroxycinnamic acid (Sigma) in 40% acetonitrile, 0.1% trifluoroacetic acid) with 1 μl of peptide (5–10 pmol). This mixture was then loaded on a stainless steel sample holder and dried at room temperature. A VG Analytical Tofspec mass spectrometer equipped with a 337-nm laser was used for sample analysis, with a 25-kV acceleration voltage. From 50 to 150 shots were accumulated for each spectrum acquisition in the positive and negative ion mode. Calibration with external standards was obtained with a mixture of peptide LWMRFA (Tebu) and insulin (Sigma) in a 1/3 concentration ratio (10-pmol total sample load) with the same matrix.

Edman Degradation—Peptides were applied to precycled Polybrene-treated glass fiber discs. Automated sequencing was done on a four-cartridge Procise 494A pulsed-liquid phase sequencer (Applied Biosystems).

Assay for GEF Activity—The dissociation rates of the Ha-Ras·[^{3}H]GDP complexes were measured kinetically at 30 °C by the nitrocellulose binding assay. The labeled Ha-Ras·[^{3}H]GDP complex was prepared by incubation of 2 μM Ha-Ras and 6 μM [^{3}H]GDP (350 Bq·pmol^{-1}, PerkinElmer Life Sciences) for 5 min at 30 °C in 100 μl of buffer B (50 mM Tris-HCl, pH 7.5, 1 mM $MgCl_2$, 100 mM NH_4Cl, and 0.5 mg·ml^{-1} bovine serum albumin) containing 3 mM EDTA. Then, 3 mM $MgCl_2$ were added. The reaction mixture (50–200 μl) for the dissociation experiments contained, in buffer B, 0.1–0.2 μM Ha-Ras·[^{3}H]GDP complex and full-length MBP-CDC25Mm, either wild-type or mutant, as indicated in legends to figures. Dissociation kinetics were started by the addition of a 500-fold excess of unlabeled nucleotide. The concentration of glycerol carried over from the CDC25Mm storage buffer was 10% maximum and was compensated by adding an equivalent amount of storage buffer to the control. At the given times, the samples (5–10 μl) were filtered through nitrocellulose discs (Sartorius 11306, 0.45 μm), washed twice with 3 ml of ice-cold buffer C (50 mM Tris-HCl, pH 7.5, 10 mM $MgCl_2$, 100 mM NH_4Cl), and the retained Ha-Ras-bound radioactivity counted.

Other Materials and Methods —Human Ha-Ras-p21 was purified as described (22). Protein concentrations were determined by [^{3}H]GDP binding for Ha-Ras and with the Bio-Rad protein assay for the other proteins, using bovine serum albumin as a standard. For a precise comparison of the concentrations of wild-type and mutant proteins, Coomassie Blue-stained gels were analyzed with the Apple scanner system and the results evaluated with Scan Analysis software. Molecular size markers for SDS-PAGE were from Amersham Pharmacia Biotech.

RESULTS

In Vitro Phosphorylation of CDC25Mm by PKA—In order to understand the mechanism by which phosphorylation of GEF could influence the activity of the downstream pathway(s), we have characterized the ability of various serine/threonine kinases to phosphorylate purified full-length CDC25Mm *in vitro*, an aspect that has yet to be investigated. Phosphorylation of CDC25Mm was examined after incubation with PKA, PKC, CKII, or CaMKII in the presence of [γ-^{32}P]ATP. After SDS-PAGE electrophoresis and autoradiography, the labeled band (Fig. 1) corresponding to full-length CDC25Mm was identified by comparison with Coomassie Blue-stained gel. In the experimental conditions chosen, each kinase was added in an amount capable of phosphorylating 300–500-fold more protein substrate than the amount of CDC25Mm present in the incubation mixtures. A pronounced phosphorylation was obtained with PKA, whereas the effects of the other three kinases was much lower, about 0.5–1% that of PKA in the case of CaMKII and even less with PKC and CKII.

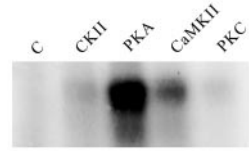

FIG. 1. **Phosphorylation of CDC25Mm by casein kinase II, PKA, calmodulin kinase II, and PKC.** CDC25Mm (2 μg) was incubated with 0.2 milliunit of CKII, 0.5 milliunit of PKA, 0.5 milliunit of CaMKII, or 0.3 milliunit of PKC in the presence of [γ-^{32}P]ATP (33 Bq/pmol) for 30 min at 30 °C in a final volume of 30 μl of appropriate buffer. The specific activity of the different kinases was 1 nmol of phosphate transferred/milliunit/min to peptide or protein substrates. Control experiments (*C*) contained buffer instead of kinase. Each sample (10 μl) was analyzed on a 10% (w/v) acrylamide SDS-PAGE followed by autoradiography.

These results led us to quantify the extent of PKA-dependent phosphorylation. Noteworthy, all of the CDC25Mm preparations used were purified in native conditions and showed a well characterized RasGEF activity. Fig. 2 reports the kinetics of the CDC25Mm phosphorylation (*A*) and the phosphate incorporation as a function of PKA (*B*) and ATP (*C*) concentrations. CDC25Mm phosphorylation reached a plateau value after 20 min of incubation in the presence of 10 milliunits of PKA and 100 μM ATP. Phosphorylation stoichiometry measurements were performed at a CDC25Mm concentration of 70 nM. Higher CDC25Mm concentrations led to a decrease of the phosphorylation stoichiometry. For example, under the same conditions (10 milliunits of PKA), the use of a 10-fold higher concentration of CDC25Mm led to a 6 times lower stoichiometry. For each labeling, special care was taken to control the specific incorporation of ^{32}P into CDC25Mm. As detailed under "Experimental Procedures," two methods were used for phosphorylation stoichiometry determination. These are, quantification of the trichloroacetic acid-insoluble radioactivity of the samples from the phosphorylating mixture, on one hand, and measurement of the radioactivity of excised CDC25Mm band from SDS-PAGE, on the other hand. The stoichiometry of phosphorylation of CDC25Mm, as determined with these two methods, represented about 4 mol of phosphate covalently incorporated/mol of CDC25Mm. For comparison, the molar stoichiometry obtained with CaMKII was 0.01–0.02.

PKA Phosphorylates CDC25Mm in Vivo—We then investigated whether PKA phosphorylation of CDC25Mm also occurs in intact cells. NIH 3T3 fibroblasts overexpressing CDC25Mm (clone NIHRG7) were treated with forskolin in order to increase cAMP level and thus activate PKA. Total cell extracts were then analyzed by Western blotting with CDC25Mm antibodies. Fig. 3*A* shows that the treatment with forskolin rapidly causes a reduction in the electrophoretic mobility of the protein, persisting at least up to 30 min. This shift in mobility is due to phosphorylation, since treatment of immunoprecipitated CDC25Mm with acidic potato phosphatase restored the higher mobility of the protein (data not shown).

A back phosphorylation experiment confirmed that PKA phosphorylates *in vivo* CDC25Mm. CDC25Mm was isolated from control cells and from cells pretreated with forskolin for

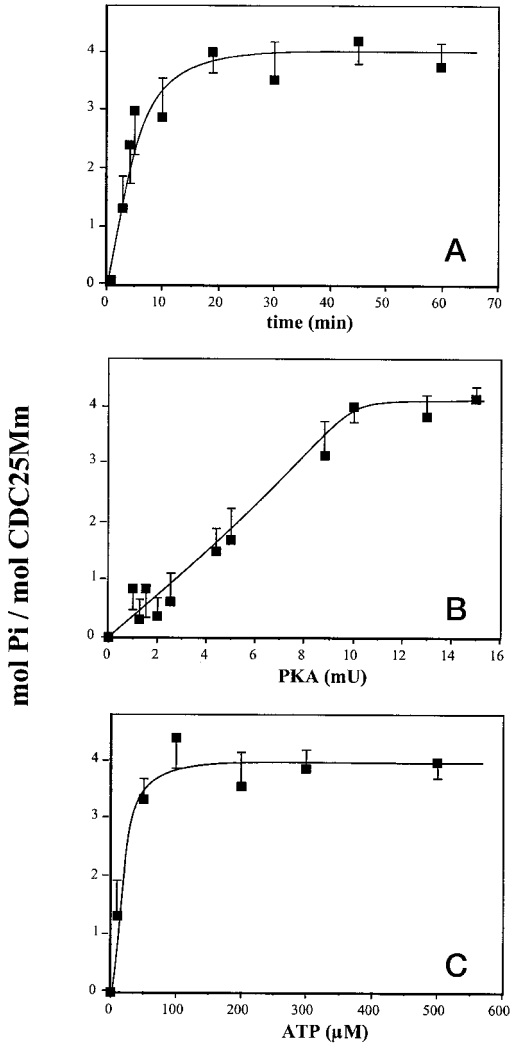

FIG. 2. **Stoichiometry of CDC25Mm phosphorylation by PKA.** CDC25Mm (70 nM) was incubated with PKA in the presence of [γ-^{32}P]ATP (33 Bq/pmol) at 30 °C, as a function of time (*panel A*) and of PKA (*panel B*) or of ATP (*panel C*) concentrations. In *A* and *C*, 10 milliunits of PKA were used; in *B* and *C*, the incubation time was 30 min. To measure the amount of phosphate incorporated, each labeled sample (15 μl) was precipitated in trichloroacetic acid as described under "Experimental Procedures."

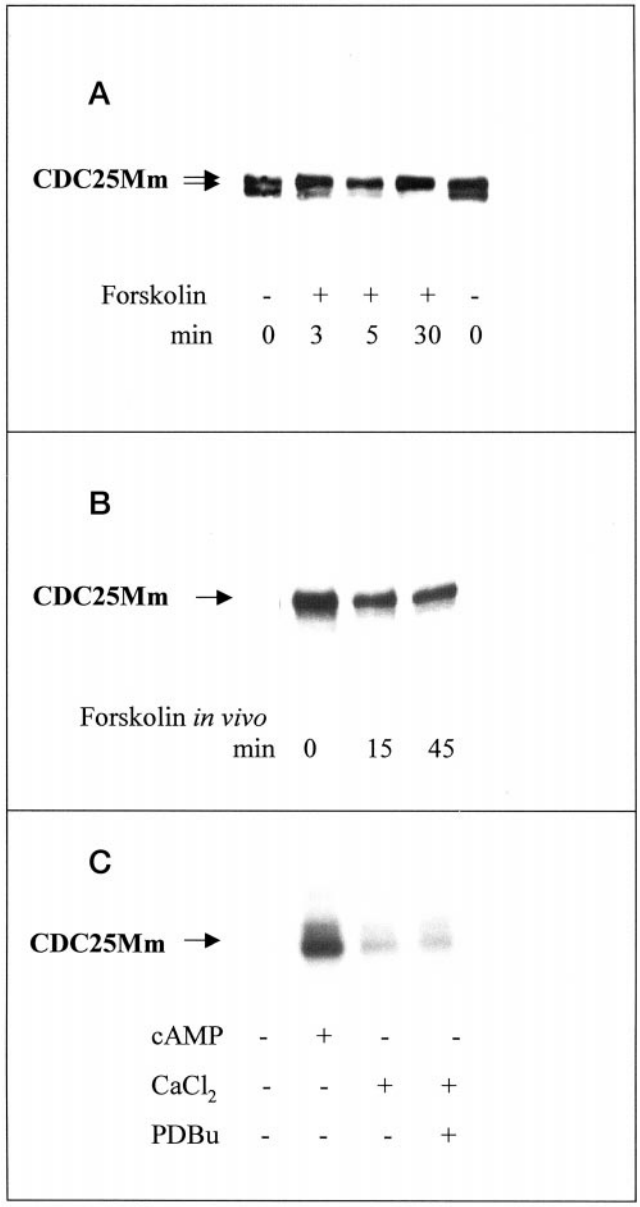

FIG. 3. **Phosphorylation of cellular CDC25Mm protein.** In *panel A*, NIH3T3 fibroblasts overexpressing CDC25Mm (clone NIHRG7, see Ref. 7) were serum-starved for 24 h, then left untreated or stimulated with 50 μM forskolin for 3, 5, or 30 min. Equal amounts of total cell extracts were analyzed in Western blotting with anti Ras-GRF antibodies. In *panel B*, serum-starved NIH3T3 fibroblasts, clone NIHRG7, were either left untreated or treated with 50 μM forskolin for 15 or 45 min. CDC25Mm was then immunoprecipitated with Ras-GRF antibodies and subjected to *in vitro* phosphorylation by protein kinase A catalytic subunit in the presence of [γ-^{32}P]ATP. The reaction mixture was then separated by electrophoresis and analyzed by autoradiography. The intensity of the bands was quantified by densitometric scanning. The relative values obtained are as follows: *first lane*, 4.98, *second lane*, 2.35, *third lane*, 2.40 arbitrary units. In *panel C*, 200 μg of mouse brain synaptosomal membranes were incubated in a phosphorylation mix containing 370 KBq of [γ-^{32}P]ATP and either the buffer alone or supplemented with 10 mM 8-Br-cAMP, 1.5 mM $CaCl_2$, or 1.5 mM $CaCl_2$ plus 200 nM PDBu. After incubation at 30 °C for 5 min, CDC25Mm was suspended in RIPA buffer, immunoprecipitated with Ras-GRF specific antibodies (Santa Cruz), and analyzed by SDS-PAGE and autoradiography.

15 and 45 min, and then subjected to *in vitro* phosphorylation by the catalytic subunit of PKA. As shown in Fig. 3*B*, the amount of [^{32}P]phosphate incorporated into CDC25Mm isolated from treated cells was much lower (40–50%) than that incorporated in CDC25Mm from untreated cells. Lowering the stoichiometry of phosphate incorporation might reflect *in vivo* phosphorylation of CDC25Mm by PKA.

We previously showed by subcellular fractionation of mouse brain that CDC25Mm is associated with synaptosomal membranes and is enriched in postsynaptic densities (25). Synaptosomal membranes contain PKA, PKC, and CaMKII (24, 25), and, under conditions allowing the activity of the different kinases, it is possible to identify endogenous physiological substrates (24). To investigate whether CDC25Mm is phosphorylated by PKA in its physiological environment, mouse brain synaptosomal membranes were isolated and incubated in a kinase assay in the presence of [γ-^{32}P]ATP without or with 8-Br-cAMP. Additionally, calcium alone or calcium and PDBu (an activator of PKC) were tested. Membranes were solubilized, and CDC25Mm was immunoprecipitated and analyzed by SDS-PAGE and autoradiography. As shown in Fig. 3*C*, 8-Br-cAMP markedly stimulated the phosphorylation of CDC25Mm in the synaptosomal membrane system, while only a very modest incorporation of [^{32}P]phosphate was observed in the presence of calcium and calcium plus PDBu. This experiment indicates that PKA can heavily phosphorylate CDC25Mm in the

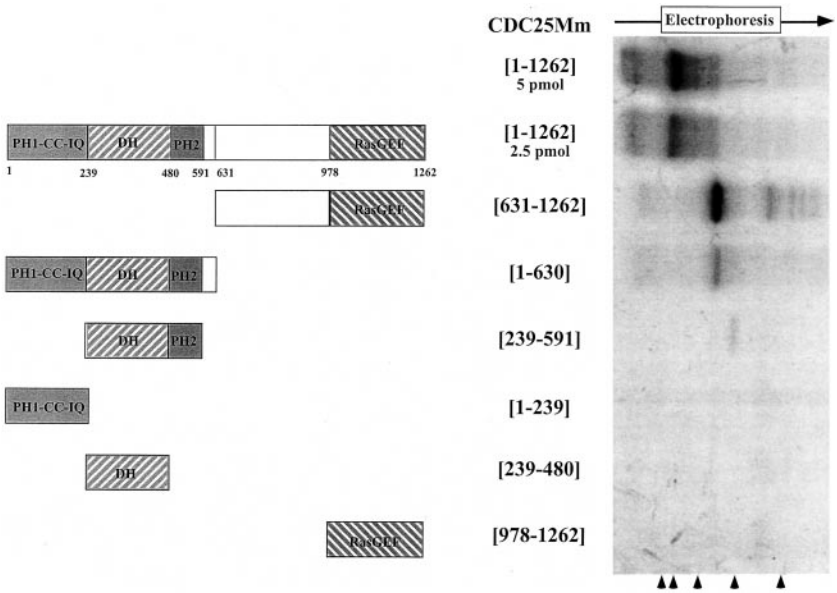

FIG. 4. **Phosphorylation of recombinant CDC25Mm proteins.** The diagram illustrates the different CDC25Mm constructs used for *in vitro* PKA phosphorylation assay, while the autoradiography shows the extent of the ^{32}P incorporation. Full-length CDC25Mm or its isolated domains were incubated, in the presence of 100 μM [γ-^{32}P]ATP, with 10 milliunits of PKA in a total volume of 25 μl at 30 °C for 30 min. After addition of 20 μl of loading buffer, a 20-μl aliquot of each sample was analyzed on a 10% (w/v) acrylamide SDS-PAGE followed by autoradiography. The same amount of protein was used for each PKA phosphorylation assay (5 pmol) except in *lane 2* (2.5 pmol of CDC25Mm-(1–1262)). *Numbering* refers to the size of the fragments of CDC25Mm, fragment 1–1262 being the full-length protein. *Arrows* indicate the position of mass markers (212, 170, 116, 76, and 53 kDa) as revealed by Coomassie Blue staining of the SDS-PAGE.

neuronal tissue, whereas other kinases (calcium/calmodulin-dependent and protein kinase C) are much less active toward this protein.

Definition of the Phosphoserine/Phosphothreonine-containing Regions—In order to characterize the PKA phosphorylation sites with respect to the various domains of CDC25Mm, different fragments of CDC25Mm (corresponding to known functional domains, such as the catalytic C-terminal domain (RasGEF domain), the RacGEF domain (DH), and various motifs, like PH and IQ) were constructed, isolated, and examined for their PKA-dependent phosphorylation. The ^{32}P-labeled proteins were visualized by autoradiography and quantified after gel band extraction. In Fig. 4, we compare the phosphorylation of the full-length molecule with that of the isolated domains. The ^{32}P incorporation in the N-terminal moiety and its shorter fragments was not significant. In addition, as revealed by autoradiography, ^{32}P incorporation in the full-length molecule was comparable to that of the C-terminal half-moiety, whereas the isolated C-terminal RasGEF domain was not a PKA substrate. These results were confirmed by quantitative measurements of the phosphorylation content (data not shown). Accordingly, the region encompassing residues 631–978 contains the major sites of phosphorylation by PKA. Thus, the phosphorylation sites were clustered in a poorly characterized region of the protein containing the REM and PEST motifs.

Identification of PKA-dependent Phosphorylation Sites on CDC25Mm—To identify the modified residues, CDC25Mm-(631–1262) phosphorylated *in vitro* by PKA was digested by trypsin. The resulting phosphopeptides were first subjected to two-dimensional fingerprinting, of which a representative map is shown in Fig. 5. Several radioactive spots were visible. The nine main spots eluted represented 28%, 20%, 15%, 10%, 8%, 6%, 4%, 3%, and 3% of the total radioactivity recovered from the thin layer plate. Three additional weak spots, each of which was not in sufficient quantity for peptide analysis, amounted together to 3% of the recovered radioactivity. Each of the nine recovered spots were further purified by reverse phase HPLC on a C18 column. Between 80% and 90% of the radioactive

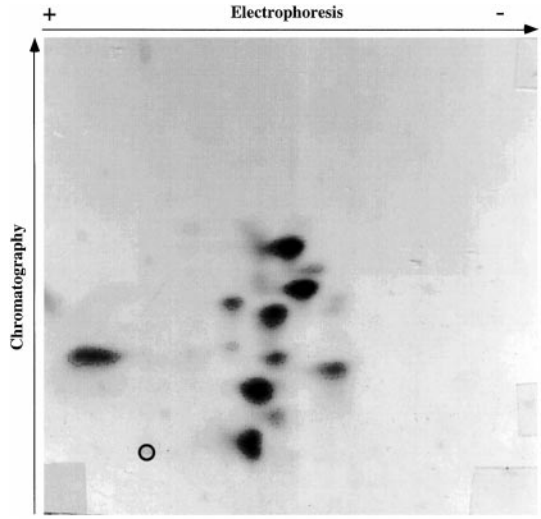

FIG. 5. **Autoradiography of the Tryptic map of ^{32}P-labeled CDC25Mm.** The tryptic peptides were resolved by electrophoresis at pH 4.4 in the first dimension and by chromatography in the second dimension. Origin (*O*) is indicated.

peptides were eluted from the column. Radioactive fractions were analyzed by MALDI mass spectrometry. Labeled peptides showed a mass increase of 80 Da, which is characteristic for peptides with single phosphorylation sites.

The molecular masses of phosphorylated peptides are listed in Table I. Seven phosphopeptides corresponding to seven discrete phosphorylation sites on CDC25Mm-(631–1262) were identified (Table I). Since the rules governing peptides desorption in MALDI mass spectrometry are not yet fully elucidated, one could not exclude that some peptides did not desorb from the matrix. Therefore, automated Edman degradation was also performed. The results are shown in Table II. The combination of MALDI and Edman degradation revealed nine phosphopeptides corresponding to serines 643, 691, 745, 793/794, 822, 849, 1123/1124, and 1146, and threonine 798.

TABLE I

Mass spectral analysis of phosphopeptide digest of PKA-phosphorylated CDC25Mm

Tryptic peptides were analyzed after reverse phase HPLC by mass spectrometry. The phosphorylated residues are underlined. In the peptides with two serines, both are underlined.

Sequence	Residues	Expected mass	Measured mass	Site(s) identified
		Da	*Da*	
YA<u>S</u>VER	641–646	724.8	722.8	Serine 643
KPM<u>S</u>AIPAR	688–696	971.2	970.4	Serine 691
LCMA<u>SS</u>LPK	789–797	950.2	949.2	Serine 793/794
<u>T</u>PEEIDVPATIPEK	798–811	1785.2	1788	Threonine 798
<u>S</u>PPTPK	849–854	626.7	625.9	Serine 849
CLHNYNAVLEIT<u>SS</u>INR	1111–1127	1948.2	1947.8	Serine 1123/1124
<u>S</u>LLDK	1146–1150	575.7	574.5	Serine 1146

TABLE II

Phosphopeptides identified by Edman degradation

Tryptic peptides were analyzed after reverse phase HPLC by Edman degradation. The phosphorylated residues are underlined.

Sequence	Residues	Site(s) identified
KPM<u>S</u>AIPAR	688–696	Serine 691
KL<u>S</u>LNIPHTGGK	743–755	Serine 745
<u>T</u>PEEIDVPATIPEK	798–811	Threonine 798
KH<u>S</u>SDVLK	820–827	Serine 822

As already mentioned, most of phosphorylated residues are clustered around the REM/PEST region, with the exception of two weakly radiolabeled sites located in the RasGEF domain (Fig. 6). It should be noted that the latter two sites were not previously identified by using the isolated RasGEF domain as substrate for the PKA experiments. The other seven sites were located between residues 643 and 849. Five PKA consensus sites are present in the primary structure of CDC25Mm (residues 83, 726, 745, 822, and 916) of which only Ser^{745} and Ser^{822} were found phosphorylated. Moreover, determination of the phosphorylation extent after thin layer fingerprinting and HPLC separation indicated the peptides containing Ser^{745} and Ser^{822} as the two major phosphorylated ones.

Effect of Phosphorylation on the RasGEF Activity and Site-directed Mutagenesis of Ser^{745} and Ser^{822}—In order to determine the functional effect of phosphorylation on the full-length CDC25Mm, we have measured the dissociation kinetics of Ha-Ras-p21·GDP in the presence of purified CDC25Mm preincubated with PKA. These experiments showed an inhibitory effect of CDC25Mm phosphorylation on the Ras nucleotide exchange but only to a modest extent (about 15% of the control values, data not shown). One should, however, stress that due to technical reasons these measurements required CDC25Mm concentrations higher than those used to obtain maximum phosphorylation (500 *versus* 70 nM). They were therefore carried out under conditions yielding around 30% of maximum phosphorylation (see first paragraph of "Results").

The observation that Ser^{745} and Ser^{822} are the residues most efficiently phosphorylated by PKA designated them as priority targets for site-directed mutagenesis. Ser^{745} and Ser^{822} were mutated in aspartate to mimic the presence of the negative charge of phosphate and in alanine, as a control measuring the effect of a substitution with an uncharged amino acid displaying only a methyl group as side chain. The four CDC25Mm mutants were purified under the same conditions as the wild-type protein. The control mutants CDC25Mm(S745A) and CDC25Mm(S822A) showed the same GEF activity on Ha-Ras as the wild-type CDC25Mm (Fig. 7*A*). The RasGEF activity of CDC25Mm(S745D) was also close to that of the wild-type factor. In contrast, the GEF activity of CDC25Mm(S822D) was much lower, corresponding to less than one third of that of the wild-type protein (Fig. 7, *A* and *B*). These results propose Ser^{822}, a residue situated in the PEST region, as a candidate for a physiological function.

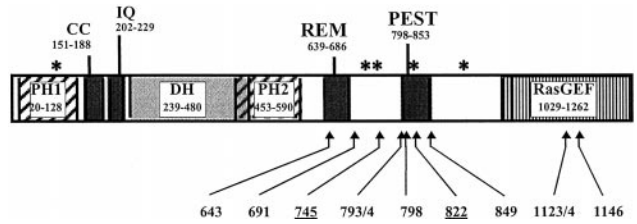

FIG. 6. **Schematic representation of PKA-phosphorylated sites in CDC25Mm.** The *numbers* indicate the limits of the known domains in CDC25Mm. PKA consensus sites (*) and phosphorylated residues (↑) are shown.

DISCUSSION

Protein phosphorylation is one of the most important mechanisms of regulation of signal transmission in the cell. It has been object of intensive investigations in the many GEFs of the Rho family, and it has recently evoked a renewed interest in the RasGEF of the CDC25Mm/GRF1 type. Even if the phosphorylation of this neuronal RasGEF and its association with the activation have been known for several years (8, 6), our knowledge of the phosphorylation sites and the biochemical mechanisms involved therein is as yet unclear. However, since treatment of the isolated exchange factor with protein phosphatase 1, specific for serine/threonine residues, abolished the ligand-induced increase in exchange activity (6), serine/threonine kinases can be expected to participate, at least in part, in the regulation of the CDC25Mm activity. This problem has been approached in this work by analyzing various serine/threonine kinases. Observations are reported, demonstrating *in vivo* and *in vitro* the selective participation of PKA in the phosphorylation of CDC25Mm and the *in vitro* identification of the PKA-dependent phosphorylation sites located in the C-terminal moiety.

A possible involvement of CDC25Mm in a PKA-dependent Ras activation had been proposed previously on the basis of the observation that in cortical neurons the level of active Ras (Ras·GTP) was strongly enhanced in response to treatment with forskolin (26). Pretreatment with H89, a specific inhibitor of PKA, reduced this activation. In this regard, it is worth mentioning that Mattingly (16) has recently reported from *in vivo* and *in vitro* experiments that phosphorylation of serine 916 was in part dependent on PKA. Phosphorylation of CDC25Mm by PKA has been shown in our work to take place in the neuronal tissue, using synaptosomal membranes from mouse brain that contain PKA, PKC, and CaMKII (24, 25). It is interesting to note that, in fibroblasts overexpressing CDC25Mm, the *in vitro* phosphorylation of CDC25Mm was decreased by 50%, following *in vivo* phosphorylation with PKA. These results strongly suggest that PKA unequivocally phosphorylates this RasGEF *in vivo*, and that the sites that are phosphorylated *in vitro* are in large part coincident with those *in vivo*.

Our *in vivo* data satisfactorily agree with those obtained *in*

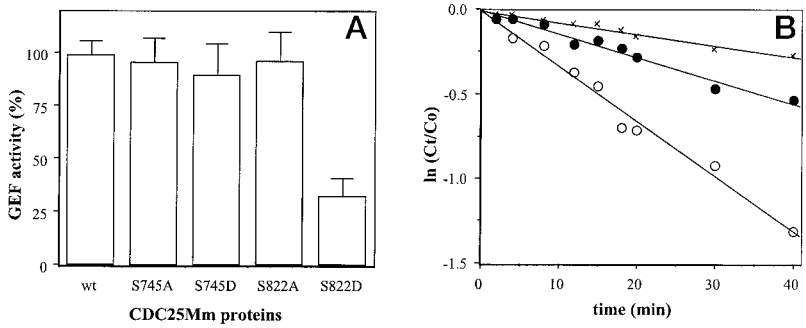

FIG. 7. **RasGEF activity of CDC25Mm mutated in position Ser^{745} and Ser^{822}.** The GEF activity of purified full-length mutated CDC25Mm proteins was determined as stimulation of the dissociation rate of the Ha-Ras-p21·GDP complexes (see "Experimental Procedures"). Several CDC25Mm preparations of either wild-type or mutants and several CDC25Mm concentrations were used to compare their specific activities. *Panel A* represents the relative GEF activities of CDC25Mm(S745A), CDC25Mm(S745D), CDC25Mm(S822A), and CDC25Mm(S822D), as percentage of the GEF activity of the wild-type product. *Panel B* shows a typical experiment determining the GEF activity of the CDC25Mm products. The dissociation rates of Ha-Ras-p21·[^{3}H]GDP complexes were measured kinetically at 30 °C using the nitrocellulose binding assay, in the absence (×) or in the presence of 200 nM CDC25Mm-wt (*white circle*) or 200 nM CDC25Mm(S822D) (*black circle*).

vitro using well characterized purified components, which indicate that several serine and threonine residues are the targets for CDC25Mm phosphorylation by PKA. The plateau value of phosphate incorporation in CDC25Mm in the presence of PKA corresponded to a stoichiometry of 4 mol of phosphate groups covalently attached/mol of full-length CDC25Mm. In buffer conditions that are optimal for the activity of PKC, CaMKII, and CKII, these kinases failed to significantly phosphorylate the full-length CDC25Mm. The catalytic C-terminal domain (285 amino acids) of CDC25Mm as well as isolated domains of the N-terminal region did not appear to contain phosphorylation sites. Accordingly, the region encompassing residues 631–978 was shown to bear most of the PKA phosphorylation sites on the exchange factor. These results were confirmed by the structural analysis of the isolated phosphopeptides by MALDI mass spectrometry and Edman degradation, which identified nine phosphorylated sites corresponding to serines 643, 691, 745, 793/794, 822, 849, 1123/1124, and 1146 and threonine 798 in the primary structure of CDC25Mm. Most of the Ser/Thr residues were clustered in the C-terminal half of the protein, in a region containing the REM (fragment 639–686) and the PEST (fragment 798–853) motifs. This region, preceding the RasGEF catalytic domain with the conserved CDC25 homology, is not well characterized as yet.

Of the nine PKA-specific phosphorylation sites identified in the present work, only two (Ser^{745} and Ser^{822}) coincided with the PKA consensus sites that we have deduced from the analysis of the CDC25Mm primary structure. The fact that these two residues were the most strongly phosphorylated made them priority candidates for site-directed mutagenesis (see below). The two weakly labeled Ser^{1123}/Ser^{1124} and Ser^{1146}, identified in the catalytic region of CDC25Mm, were not found phosphorylated in the isolated C-terminal catalytic domain, suggesting that their accessibility to PKA can be influenced by the presence of the other domains. Ser^{1146} is not conserved in human GRF1, whereas both Ser^{1123} and Ser^{1124} are conserved in murine, rat, and human GRF1. In CDC25Mm, substitution of Ser^{1124} has been reported to influence the GEF activity (27). The adjacent Ser^{1123} is homologous to SOS Ala^{877}, which in the three-dimensional model hydrogen-bonds Gln^{70} of Ha-Ras (28), a residue situated on α-helix 2 of the switch 2 region that is essential for the exchange reaction (29, 30). A phosphorylated residue, Ser^{643}, was identified in the REM sequence, a conserved stretch essential for the function and structural integrity of the RasGEF family. Ser^{643} is homologous to SOS residue Leu^{609}, which, in the three-dimensional model, interacts with the RasGEF domain of SOS (28). The other phosphorylated serines (residues 691, 745, 793/794, 798, 822, and 849) are clustered around the PEST motifs in the most divergent region of GRF1 and GRF2, in which the weak homology is associated with a variable extension of the PEST motifs. Of these residues, serine 798 is not conserved whereas residues 793/794 and 822 are conserved in all known GRF1 but not in GRF2, like Ser^{916}. It is possible that they have a regulatory function specific for GRF1. Worth mentioning, GRF1 and GRF2 are very similar in the primary structure, but different in tissue specificity. Even though residues 691, 745, and 849 are located in a very diverging region, they are serines or threonines in CDC25/GRF1Mm, GRF1rat, GRF1Hs, GRF2Mm, and GRF2Hs. This observation makes it likely that these residues play a functional role such as the interaction with as yet unidentified ligands.

PEST motifs are known in a number of cases to constitute targets of signals for proteolytic events (31). In the case of CDC25Mm, its *in vitro* treatment with the Ca^{2+}-dependent protease calpain was found to lead to the production of C-terminal fragments cleaved in the region of the REM/PEST motifs (13). However, so far, no data have been reported about the half-life of CDC25Mm in the neuronal cell. In this regard, we would like to mention that a newly discovered subclass of evolutionary conserved Ras-like protein, κB-Ras, has recently been shown to interact specifically with a PEST region of the protein ligand IκBβ, decreasing its proteolytic degradation (32). Noteworthy is also the observation that *S. cerevisiae* GEFs Cdc25p and Sdc25p display short half-lives in the yeast cell (33).

Phosphorylation of Ser^{916}, which is in part dependent on the action of PKA (16), has not been identified in our study. The PKA-dependent phosphorylation of this residue was reported not to induce any relevant effect on the RasGEF activity, whereas the carbachol-dependent phosphorylation of the same residue by an as yet unidentified kinase was necessary for full activation of the exchange factor *in vivo*. It is probable that the minor importance of the PKA action together with differences in the *in vitro* approach (in the case of Mattingly (Ref. 16), a short GRF1 fragment of 83 amino acid residues was used) justifies the discrepancy.

An important point, that remains to be assessed, is the effect of the PKA-dependent phosphorylation of the RasGEF activity of CDC25Mm. From the results *in vivo* reported by Mattingly and Macara (16), we were expecting a stimulation of the GEF activity of CDC25Mm. However, we could only observe that *in vitro* phosphorylation of CDC25Mm induces a slight inhibition of the GDP dissociation rate from the Ha-Ras·GDP complex. As already mentioned, this result could be, at least in part, the consequence of the lower phosphorylation efficiency obtained

under the conditions required for the functional test. More impressive was the 70% inhibition that we detected by substituting Ser^{822} with aspartate, a mutation mimicking the negative charge of the phosphate. In contrast, no effect was obtained by replacing Ser^{745} with aspartate. One should here stress that our analysis, as in most reports dealing with the functional analysis of RasGEF residues, was limited to the function leading to the stimulation of the exchange on Ras proteins. It is possible that Ser^{745} is involved in other functions not identified as yet. We would like to mention that CDC25Mm has been involved in the mechanisms of long term memory (34, 35) and has been reported to be an important postnatal regulator of the synthesis and release of growth hormone (36). The detailed analysis of all the combinations of residues susceptible of phosphorylation *in vitro* would doubtless contribute to a better comprehension of their functions.

Recently, Kiyono *et al.* (18) have shown that GRF1 can also be phosphorylated by the nonreceptor kinase Src. This modification slightly enhanced the exchange activity on Rac1, a member of the Rho family of GTPases. In contrast, no effect on the RasGEF activity of GRF1 was observed. Altogether, these observations suggest a very complex situation for the regulation of CDC25Mm/GRF1 activity(ies) by phosphorylating events, in which more than one kind of kinases and several pathways are likely to be involved. The fine tuning of switch molecules like Ras proteins, which are central elements of pathway networks, makes reasonable the existence of several regulatory mechanisms, in which GEF, the factor responsible for the regeneration of the active form of Ras, can be expected to be one of the most important component involved.

Acknowledgment—We are indebted to M. J.-B. Créchet for advice and helpful comments on the manuscript.

REFERENCES

1. Shields, J. M., Pruitt, K., McFall, A., Shaub, A., and Der, C. J. (2000) *Trends Cell Biol.* **10,** 147–154
2. Cherfils, J., and Chardin, P. (1999) *Trends Biochem. Sci.* **24,** 306–311
3. Schlessinger, J. (1993) *Harvey Lect.* **89,** 105–123
4. Ebinu, J., Bottorff, D., Chan, E., Stang, S., Dunn, R., and Stone, J. (1998) *Science* **280,** 1082–1086
5. Tognon, C. E., Kirk, H. E., Passmore, L. A., Whitehead, I. P., Der, C. J., and Kay, R. J. (1998) *Mol. Cell. Biol.* **18,** 6995–7008
6. Mattingly, R., and Macara, I. (1996) *Nature* **382,** 268–272
7. Zippel, R., Orecchia, S., Sturani, E., and Martegani, E. (1996) *Oncogene* **12,** 2697–2703
8. Farnsworth, C., Freshney, N., Rosen, L., Ghosh, A., Greenberg, M., and Feig, L. (1995) *Nature* **376,** 524–527
9. Buchsbaum, R., Telliez, J. B., Goonesekera, S., and Feig, L. A. (1996) *Mol. Cell. Biol.* **16,** 4888–4896
10. Fam, N. P., Fan, W. T., Wang, Z., Zhang, L. J., Chen, H., and Moran, M. F. (1997) *Mol. Cell. Biol.* **17,** 1396–1406
11. de Hoog, C. L., Fan, W. T., Goldstein, M. D., Moran, M. F., and Koch, C. A. (2000) *Mol. Cell. Biol.* **20,** 2727–2733
12. Anborgh, P. H., Qian, X., Papageorge, A. G., Vass, W. C., DeClue, J. E., and Lowy, D. R. (1999) *Mol. Cell. Biol.* **19,** 4611–4622
13. Baouz, S., Jacquet, E., Bernardi, A., and Parmeggiani, A. (1997) *J. Biol. Chem.* **272,** 6671–6676
14. Corbalan Garcia, S., Margarit, S., Galron, D., Yang, S., and Bar-Sagi, D. (1998) *Mol. Cell. Biol.* **18,** 880–886
15. Zippel, R., Balestrini, M., Lomazzi, M., and Sturani, E. (2000) *Exp. Cell Res.* **258,** 403–408
16. Mattingly, R. R. (1999) *J. Biol. Chem.* **274,** 37379–37384
17. Kiyono, M., Satoh, T., and Kaziro, Y. (1999) *Proc. Natl. Acad. Sci. U. S. A.* **96,** 4826–4831
18. Kiyono, M., Kaziro, Y., and Satoh, T. (2000) *J. Biol. Chem.* **275,** 5441–5446
19. Innocenti, M., Zippel, R., Brambilla, R., and Sturani, E. (1999) *FEBS Lett.* **460,** 357–362
20. Nimnual, A. S., Yatsula, B. A., and Bar-Sagi, D. (1998) *Science* **279,** 560–563
21. Fan, W., Koch, C., de Hoog, C., Fam, N., and Moran, M. (1998) *Curr. Biol.* **8,** 935–938
22. Jacquet, E., Baouz, S., and Parmeggiani, A. (1995) *Biochemistry* **34,** 12347–12354
23. Ferrari, C., Zippel, R., Martegani, E., Gnesutta, N., Carrera, V., and Sturani, E. (1994) *Exp. Cell Res.* **210,** 353–357
24. Wang, J. K., Walaas, S. I., Sihra, T. S., Aderem, A., and Greengard, P. (1989) *Proc. Natl. Acad. Sci. U. S. A.* **86,** 2253–2256
25. Sturani, E., Abbondio, A., Branduardi, P., Ferrari, C., Zippel, R., Martegani, E., Vanoni, M., and Denis-Donini, S. (1997) *Exp. Cell Res.* **235,** 117–123
26. Ambrosini, A., Tininini, S., Barassi, A., Racagni, G., Sturani, E., and Zippel, R. (2000) *Mol. Brain Res.* **75,** 54–60
27. Carrera, V., Moroni, A., Martegani, E., Volponi, C., Cool, R. H., Alberghina, L., and Vanoni, M. (1998) *FEBS Lett.* **440,** 291–296
28. Boriack-Sjodin, P. A., Margarit, S. M., Bar-Sagi, D., and Kuriyan, J. (1998) *Nature* **394,** 337–343
29. Crechet, J. B., Bernardi, A., and Parmeggiani, A. (1996) *J. Biol. Chem.* **271,** 17234–17240
30. Quilliam, L. A., Hisaka, M. M., Zhong, S., Lowry, A., Mosteller, R. D., Han, J., Drugan, J. K., Broek, D., Campbell, S. L., and Der, C. J. (1996) *J. Biol. Chem.* **271,** 11076–11082
31. Rechsteiner, M., and Rogers, S. W. (1996) *Trends Biochem. Sci.* **21,** 267–271
32. Fenwick, C., Na, S. Y., Voll, R. E., Zhong, H., Im, S. Y., Lee, J. W., and Ghosh, S. (2000) *Science* **287,** 869–873
33. Kaplon, T., and Jacquet, M. (1995) *J. Biol. Chem.* **270,** 20742–20747
34. Brambilla, R., Gnesutta, N., Minichiello, L., White, G., Roylance, A. J., Herron, C. E., Ramsey, M., Wolfer, D. P., Cestari, V., Rossi-Arnaud, C., Grant, S. G., Chapman, P. F., Lipp, H. P., Sturani, E., and Klein, R. (1997) *Nature* **390,** 281–286
35. Orban, P. C., Chapman, P. F., and Brambilla, R. (1999) *Trends Neurosci.* **22,** 38–44
36. Itier, J. M., Tremp, G. L., Leonard, J. F., Multon, M. C., Ret, G., Schweighoffer, F., Tocque, B., Bluet-Pajot, M. T., Cormier, V., and Dautry, F. (1998) *Nature* **393,** 125–126

Sites of Phosphorylation by Protein Kinase A in CDC25Mm/GRF1, a Guanine Nucleotide Exchange Factor for Ras

Soria Baouz, Eric Jacquet, Katia Accorsi, Codjo Hountondji, Monica Balestrini, Renata Zippel, Emmapaola Sturani and Andrea Parmeggiani

J. Biol. Chem. 2001, 276:1742-1749.
doi: 10.1074/jbc.M005770200 originally published online October 3, 2000
